Summary of Plasma Injector Development and Free-Running Arc Experiments for a 7 km/s Plasma-Driven Railgun

F. Stefani, D. Wetz, J. V. Parker, and I. R. McNab

Institute for Advanced Technology
The University of Texas at Austin

October 2007

IAT.R 0467

Award No. FA9550-05-1-0341 with the Air Force Office of Scientific Research

No clearance required for AFOSR MURI sponsored projects

Report Documentation Page

Form Approved
OMB No. 0704-0188

1. REPORT DATE	2. REPORT TYPE	3. DATES COVERED
29 OCT 2007	**Summary**	**29 OCT 2006 - 29 OCT 2007**

4. TITLE AND SUBTITLE	5a. CONTRACT NUMBER
Summary of Plasma Injector Development and Free-Running Arc Experiments for a 7 km/s\ Plasma-Driven Railgun	5b. GRANT NUMBER **Award No. FA9550-05-1-0341**
	5c. PROGRAM ELEMENT NUMBER
6. AUTHOR(S) **F. Stefani, D. Wetz, J. V. Parker, and I. R. McNab**	5d. PROJECT NUMBER
	5e. TASK NUMBER
	5f. WORK UNIT NUMBER
7. PERFORMING ORGANIZATION NAME(S) AND ADDRESS(ES) **Institute for Advanced Technology The University of Texas at Austin 3925 W Braker Lane STE 400 Austin TX 78759-5316**	8. PERFORMING ORGANIZATION REPORT NUMBER **IAT.R 0467**
9. SPONSORING/MONITORING AGENCY NAME(S) AND ADDRESS(ES) **Air Force Office of Scientific Research 801 N Randolph ST Rm 732 Arlington, Virginia 22203-1977**	10. SPONSOR/MONITOR'S ACRONYM(S) **AFOSR**
	11. SPONSOR/MONITOR'S REPORT NUMBER(S)

12. DISTRIBUTION/AVAILABILITY STATEMENT
Approved for public release, distribution unlimited

13. SUPPLEMENTARY NOTES
No clearance required for AFOSR MURI sponsored projects., The original document contains color images.

14. ABSTRACT
The objective of the Institute for Advanced Technology (IAT) effort is to demonstrate 7 km/s with a plasma-driven railgun. Our principal challenge is to manage restrike arcs, which in past experiments have limited muzzle speeds to between 5 and 6 km/s. Restrike arcs are a consequence of ablation of the bore insulators. Our approach is to eliminate bore ablation by using: 1. high-purity alumina insulators to raise the ablation resistance of the bore, 2. pre-acceleration to prevent ablation of the bore materials at low velocity, and 3. magnetic augmentation to reduce power dissipation in the plasma. Each of these measures requires a dedicated hardware subsystem. In 2006, we designed and built the three subsystems and successfully tested the first two.

15. SUBJECT TERMS
plasma-driven railgun, restrike arcs, muzzle speeds, restrike arcs, bore insulators.

16. SECURITY CLASSIFICATION OF:			17. LIMITATION OF ABSTRACT	18. NUMBER OF PAGES	19a. NAME OF RESPONSIBLE PERSON
a. REPORT **unclassified**	b. ABSTRACT **unclassified**	c. THIS PAGE **unclassified**	**SAR**	**18**	

Table of Contents

Table of Figures

Table of Figures: Appendix A

Table of Figures: Appendix B

Table of Figures: Appendix C

Summary of Plasma Injector Development and Free-Running Arc Experiments for a 7 km/s Plasma-Driven Railgun

F. Stefani, D. Wetz, J. V. Parker, and I. R. McNab
Institute for Advanced Technology, The University of Texas at Austin

1. Introduction

The objective of the Institute for Advanced Technology (IAT) effort is to demonstrate 7 km/s with a plasma-driven railgun. Our principal challenge is to manage restrike arcs, which in past experiments have limited muzzle speeds to between 5 and 6 km/s. Restrike arcs are a consequence of ablation of the bore insulators. Our approach is to eliminate bore ablation by using:

1. high-purity alumina insulators to raise the ablation resistance of the bore,
2. pre-acceleration to prevent ablation of the bore materials at low velocity, and
3. magnetic augmentation to reduce power dissipation in the plasma.

Each of these measures requires a dedicated hardware subsystem. In 2006, we designed and built the three subsystems and successfully tested the first two.

2. Progress in 2006

In the first year of the contract (a six-month duration), we performed system-level trade studies and developed a detailed design of the launcher core, as reported in the first annual report. This year, we built and tested two of the three subsystems—the core and the pre-accelerator—and have designed and built but have not yet tested the third—the augmentation subsystem. We tested the railgun core using free-running arcs rather than projectiles, as the latter would have required integrating the three subsystems. Our tests allowed us to verify that the high-purity alumina insulator tiles can withstand the plasma and magnetic pressures for which they were designed, and our estimate of the ablation threshold is conservative, which means we can expect a greater margin for operating without ablation in the projectile experiments yet to come. We also designed, built, and tested a pre-accelerator. We were able to achieve projectile velocities of 800 m/s and are currently making modifications to achieve the desired velocity of 1000 m/s. Details of the work performed at the IAT between August 2005 and August 2006 are summarized below.

2.1. Railgun Core Subsystem

In 2006, we procured, built, and tested the core of the launcher. The core, shown in Figure 1, consists of inner rails, augmenting rails, bore insulators made of high-purity alumina, and other insulators made of G-10. A key feature of the design is the use of a long polyolefin sheath which functions to allow the bore to be evacuated and to keep the plasma from arcing over from the inner rails to the augmenting rails. An objective of our core design was to provide sufficient preload to keep the bore sealed against an estimated 100 MPa (15 ksi) peak plasma pressure

while minimizing tensile stress on the alumina tiles. A second objective was a core that did not have to be rebuilt between shots.

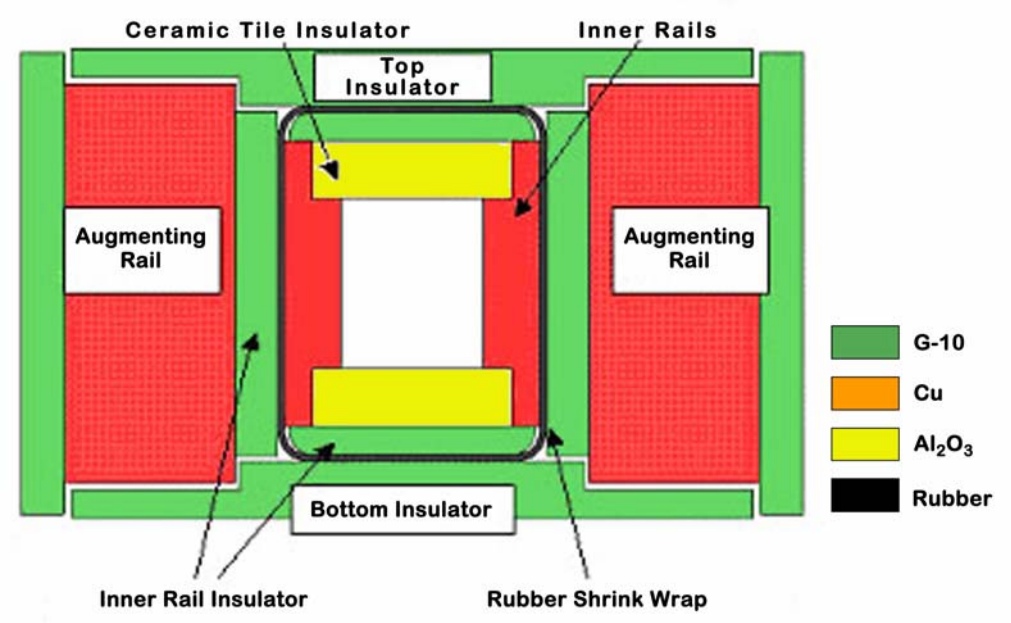

Figure 1. Cross section of the core design.

In 2006, we procured 150 tiles of 99.5% pure alumina from CoorsTek (1"×5/16"×6" with ± 0.001" on critical tolerances). A 12-foot long section of the core was assembled using these tiles and tested in a series of nine tests using free-running arcs. The tests are summarized in Appendix A. The tests demonstrated that:

- The tiles can withstand the magnetic and plasma pressures.
- Our estimate of the ablation threshold for the alumina tiles is conservative, thereby providing us with a greater margin for operating without ablation in the projectile experiments yet to come. The details of how we arrived at this conclusion are summarized in Appendix B.
- The polyolefin sheath is not damaged by the plasma, and the core does not need to be rebuilt between shots.
- Our B-dot probes, which were designed for use with solid armatures, work well with plasma armatures, even at the relatively low currents used in our experiments.

2.2. Projectile Pre-injector Subsystem

The second major subsystem is a pre-injector for the projectile; its function is to accelerate a 7 g polycarbonate projectile to 1000 m/s. Pre-acceleration is necessary in plasma-armature launchers because the effects of slow-moving arcs are quite damaging to bore components. In fact, operating without ablation is not possible below a certain threshold speed, which is a function of the material properties. For our experiment, this threshold is about 700 m/s. We have chosen to use a plasma-driven injector rather than a one-stage light-gas gun to limit the amount of gas in the railgun bore. Past experiments have shown that excessive gas from a light-gas-gun pre-injector can also lead to restrike arcs at the breech.

Our plasma injector, shown in Figure 2, is similar to plasma-source capillary generators used in electrothermal chemical (ETC) launchers. It consists of a 23 cm long, 20 mm inner diameter polyethylene liner contained within a steel pressure vessel. An exploding wire of 0.001" diameter aluminum initiates a discharge that vaporizes a controlled amount of polyethylene from the liner. In 2006, we fabricated and tested a plasma-driven pre-accelerator and demonstrated reliable operation to 800 m/s. To achieve this performance we had to build a dedicated capacitor-driven power supply. (The details of the plasma generator, the power supply, and results of the tests are described in Appendix C.)

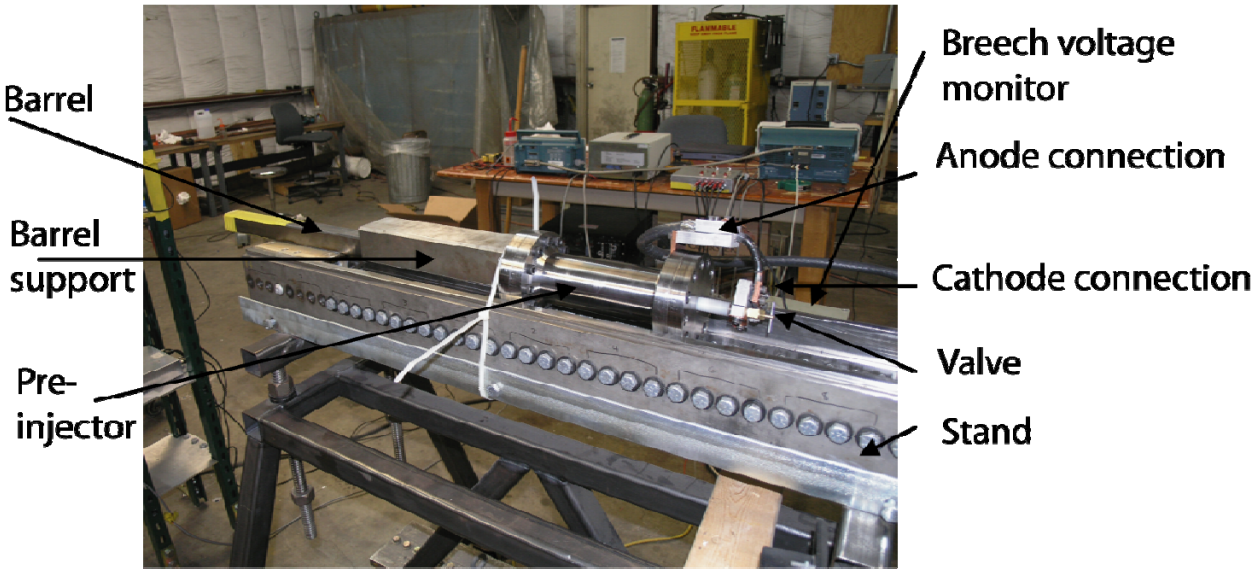

Figure 2. Pre-injector system was built and successfully tested in 2006.

2.3. Magnetic Augmentation Subsystem

In 2006, the hardware needed to build the augmenting system was designed and built. The augmentation system is straightforward, consisting of a set of rails, a cross-over at the muzzle, and hardware to react the axial and bursting forces acting on the cross-over. The augmentation hardware for the muzzle end of the rails is shown in Figure 3. The first step in testing the augmentation hardware is to ensure that the breech can withstand the voltage that will be induced when the augmenting turn is energized. We estimate this will be about 6–7 kV. In 2006, we performed a hi-pot test of the breech, which indicated some breakdown at around 4 kV. To resolve this problem, we need to disassemble, clean, and rebuild the breech, replacing any hardware that has been damaged by surface arc tracking. We plan to do this work in the fall of 2006.

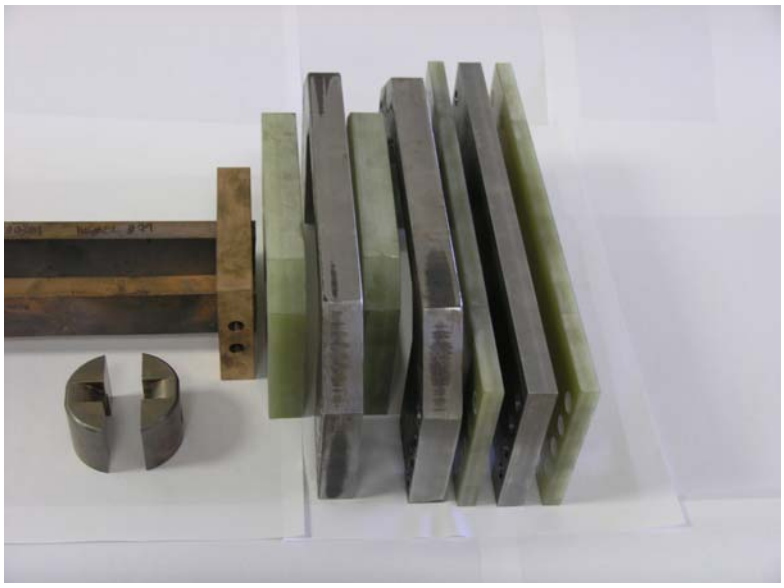

Figure 3. The augmentation subsystem hardware was designed and fabricated in 2006. Testing is scheduled for fall 2006.

3. Objectives and Milestones for 2007

In 2007, we plan to complete commissioning the three principal subsystems and integrate the subsystems so that we can begin testing with projectiles.

The work that remains to be done on the ***core subsystem*** is to fabricate and test a vacuum-tight breech section that connects the inner rails to the pre-injector and to the capacitor banks that power the inner rails.

Testing the ***augmentation subsystem*** requires that we rebuild the MCL breech to stand off 8 kV. Once that is accomplished, we will assemble and pulse the augmenting rails and cross-over hardware to ensure that the conductors can withstand the forces associated with operating at 800 kA.

The ***plasma injector*** currently operates well; however, the peak injection speed of 800 m/s is at the low end of the desirable range. We plan to modify the injector to achieve 1,000 m/s by using a longer plasma chamber and a longer drift section.

Once this work is completed, the three subsystems will be integrated and we will begin accelerating projectiles. Initial testing will be conducted using a half-length (3 m) version of the launcher. The principal advantage of working with a short launcher is that it will reduce the time needed to assemble the core and allow more time for debugging the experiment. After we reach the operating limits of the 3 m gun, we will work with the full-length launcher (7 m).

Appendix A: Summary of Free Arc Tests

The technique of using free-running arcs in a railgun was developed by Parker et al. at Los Alamos National Laboratory in the mid-1980s. The technique consists of accelerating a plasma armature down the bore of the railgun pushing against a gas prefill rather than a solid projectile. We used this technique because it allowed us to test the railgun without having to use the pre-acceleration and augmentation subsystems, which are still being developed. Because the bore gas ahead of the armature is considerably lighter than a projectile, the technique allows high velocities to be attained with relatively low currents. Arcs are initiated by vaporizing a stationary fuse in the breech of the launcher. The rapid acceleration of the arcs allows the gun to be operated below the ablation threshold of the insulators.

In June 2006, we conducted nine tests using free-running arcs in a bore filled with atmospheric pressure air. Test conditions and results are summarized in Table AI. With each successive test, we increased the current. In test 6, we achieved the design condition of 180 kA. Test 7 was conducted at just below 220 kA (that is, at 120 percent of the design condition for current). Tests 8 and 9 were similar to tests 6 and 7, except that the bore contained a helium backfill to increase the velocity of the free-running arcs. The Table A1 shows the peak currents and peak arc velocities attained in the tests. The measured arc velocities were obtained by computing $\Delta x / \Delta t$ between peaks in the B-dot traces.

Table AI. Summary of Free Arc Tests

Number	Peak Current Measurement [kA]	Peak Velocity Measurement [km/s]	Peak F_{ratio}	Comments
1	29	n/a	0.54	One bank
2	53	1. 08	0.66	One bank
3	77	1.65	0.71	One bank
4	73	1.72	0.75	Two banks, stagger fired
5	111	2.58	0.87	One bank
6	176	2.86	1.29	Two banks, fired simultaneously
7	217	3.75	1.54	Two banks, fired simultaneously
8	170	7.0	0.94	(partial) helium backfill
9	216	6.7	1.04	(partial) helium backfill

The velocities measured in tests 8 and 9 are significantly higher than those measured in tests 6 and 7. This is to be expected, because the last two tests were conducted with a helium backfill. Test 8, at 170 kA, produced a higher peak speed than test 9, at 216 kA. This result suggests that the helium backfill was not complete, and that there was more residual air in the bore for test 9 than for test 8.

The column labeled F_{ratio} is the computed heat loading incident upon the alumina tiles divided by the assumed threshold value for ablation of 12 $MWs^{1/2}/m^2$. The table shows that test 7 exceeded the assumed ablation threshold by 50%. In Appendix B, we analyze this test and find no evidence of ablation—from which we conclude that our assumed ablation threshold for

alumina is conservative. The significance of this result is that we can expect a greater margin for operating without ablation in the projectile experiments yet to come.

The free arc tests provided several other useful results. The tests showed that the gun could be fired multiple times without cracking the tiles or damaging the polyolefin sheath. When the core was disassembled and the tiles and rails were inspected for damage after the tests, most of the tiles were intact, as shown in Figure A1. The few tiles that were damaged appear to have become damaged either in the last test or during disassembly. This conclusion is based on the absence of carbon/copper deposits on the broken surfaces of the tiles.

The absence of discoloration on the edges of all tiles indicates that the core remained sealed against the plasma pressure. The polyolefin sheath, which lies outside the tiles, did not show signs of damage or exposure to the plasma, as shown in Figure A2.

Figure A1. Typical condition of the alumina tiles after the nine free arc tests.
The central portion has become discolored from exposure to the plasma armature.
The edges of the tiles are white, indicating that the bore remained sealed against the plasma pressure.

Figure A2. The breech end of the launcher, shown with the top containment and most of the top G-10 insulators removed. The exposed copper conductors are the augmenting turns, which were not energized in these tests. The black material between the augmenting turns is the polyolefin tubing that contains the inner core of the launcher (that is, the inner rails and alumina insulators). The polyolefin tubing remained intact throughout the testing.

A final result from the free arc tests was that the existing suite of diagnostics on the MCL proved usable for this experiment. B-dot probes designed for use with solid armatures—the green cards in Figure A3—worked well, even at the relatively low currents used in our experiments.

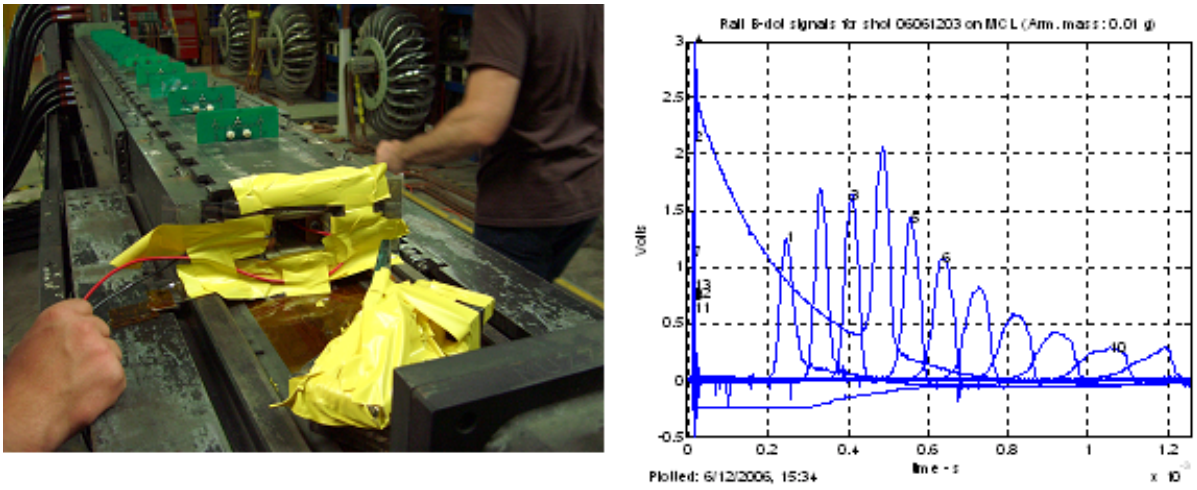

Figure A3. Photograph of the free arc experiments (left) as seen from the muzzle end of the launcher. The green cards shown in the photograph contain small loops that sense the passage of the armature. Although the cards were designed for use with solid armatures at currents on the order of 106 A, they performed well even at the relatively low currents used in these tests. The plot on the left is an overlay of all the B-dot signals from test number seven. (The anomalous signal from B-dot #4 was caused by a grounding problem.)

Appendix B: Estimate of Ablation Threshold Based on Analysis of Free Arc Test 7

A benefit of the free-running arc technique is that it provides a means to detect the onset of ablation of the insulators. From the structure of the B-dot probe signals, one can determine the length of the plasma. This appendix presents an analysis of free arc test 7, the most energetic test in air, which produced a peak bore heat flux that exceeded by 50% the assumed ablation threshold for 99.5% pure alumina. We computed the length of the arc and, more importantly, the length of the trailing edge of the arc to determine whether the arc grew from entrainment of ablation products. Our analysis finds that the trailing edge of the arc remained compact, from which we conclude that the alumina tiles did not ablate. We also find that the increase in the length of the arc is consistent with the amount of swept-up bore gas.

Figure B1 shows a waterfall plot of the data from test 7, a replot of the B-dot signals from test 7 that were shown in Figure A3 with a vertical displacement that corresponds to the axial location of each B-dot probe. We have carefully plotted and tabulated four times associated with each trace and joined them together with trajectory lines, labeled as follows:

- ***Trailing edge*** is the time when the signal rejoins the baseline
- ***Trailing 50%*** is half amplitude on the falling edge
- ***Leading 50%*** is half amplitude on the rise
- ***Leading edge*** is the first point where the signal separates from the baseline

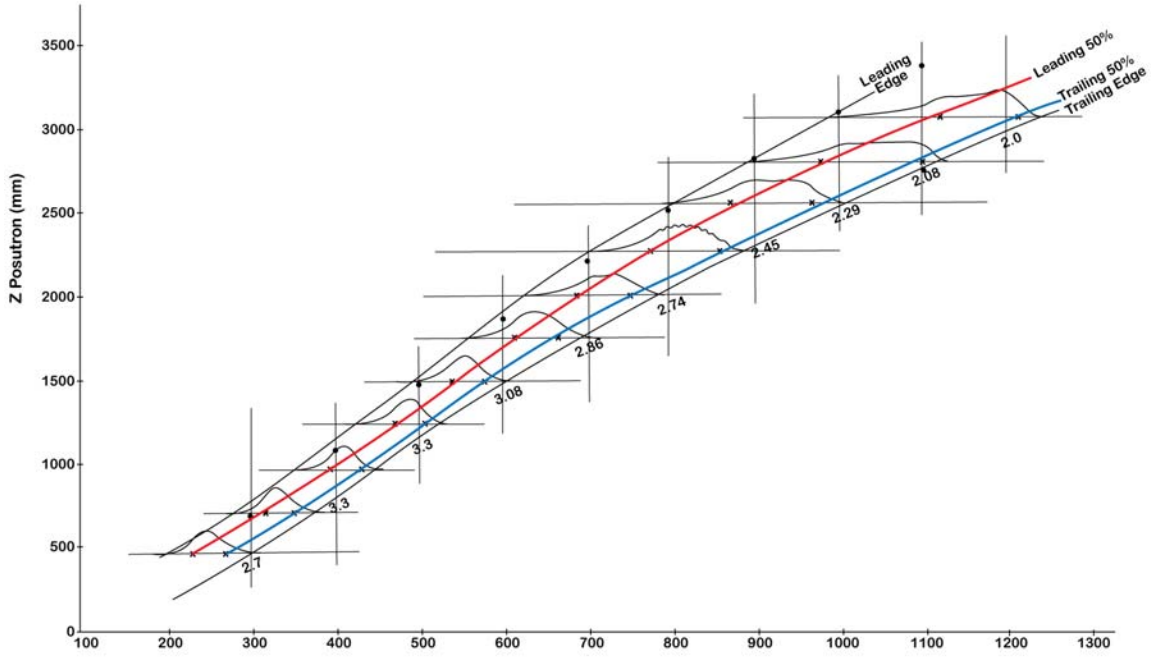

Figure B1. Waterfall plot of the B-dot traces from free arc test 7.

A vertical line at any given time represents an instantaneous measurement of the arc length. For example, at 300 μs, the distance from the trailing edge to the 50% trailing point is 77 mm. We call this distance the *tail length*. Similarly, the distance between the lead 50% point and the trailing 50% point is designated *FWHM*, and the region from the leading 50% point to the leading edge is the *precursor*.

The connection between these regions and the physical structure of the plasma/gas system in the bore is shown in Figure B2.

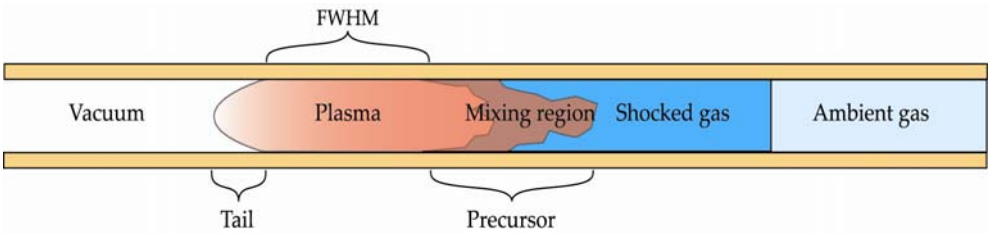

Figure B2. Schematic showing the physical structure of the plasma–gas region in a free-arc experiment and the relationship to the regions shown in Table B1.

Table BI lists the measured values of tail length, *FWHM*, and precursor length for test 7 at 100 μs intervals from 300 μs to 1200 μs.

Table BI. Measurements of the Plasma Length as a Function of Time

Time	Tail Region	FWHM	Precursor Region	Shock Front
300 μs	77 mm	109 mm	115 mm	93 mm
400	65	118	152	142
500	60	132	186	207
600	67	154	222	258
700	65	202	222	320
800	64	234	228	370
900	57	234	230	415
1000	50	234	260	453
1100	57	214	-	485
1200	59	204	-	518

The plasma acts as a piston that pushes the bore gas ahead as it moves. Because the plasma velocity is much greater than the sound speed in air (~300 m/s), a shock front is formed that travels ahead of the plasma approximately 17% faster than the plasma velocity. As this is a strong shock front with a Mach number of about 10, we know that the ambient gas is compressed by a factor of $(\gamma + 1)/(\gamma - 1)$, where $\gamma = 1.4$ for air. At a Mach number of 10, shock heating of the compressed gas is not strong enough to ionize the air, so this compressed gas region is nonconductive.

From past railgun experiments, we know that the plasma length is initially three to five times the bore height. Shorter plasma armatures are not seen, apparently due to lack of stability. For these experiments, this predicts a minimum *FWHM* value of 50–85 mm.

As the plasma/gas region moves along the bore, some turbulent mixing occurs due to wall friction. Some of the compressed gas is ionized as it mixes into the plasma and causes the plasma length to increase. Some of the ionized gas from the plasma is also mixed in the compressed gas, causing it to become partially conducting. This mixed region creates the precursor conduction.

Finally, there is the interface at the back edge of the plasma, the *tail region*. In an ideal railgun, there is a nearly perfect vacuum behind the plasma armature. Any residual gas is ionized by a combination of radiation and the high electric field. Once ionized, it is quickly accelerated and merged into the armature. When ablation is present, however, the tail region becomes very complex. Large quantities of neutral gas are vaporized into the bore. Ionization becomes inefficient, the drag forces increase, and the gas is not merged into the plasma armature. The result is an extended region of conduction behind the armature and eventually the formation of a secondary arc trailing behind the armature, often at a distance of tens of bore heights. The absence of this trailing conduction is firm evidence that ablation is weak or absent.*

Although the accuracy of these numbers is not particularly high—on the order of ± 10 mm—the trends in the data are evident. The tail length is essentially constant at 62 ± 7 mm, convincing evidence that the ablation threshold of the insulator has not been exceeded. The measured FWHM shows the plasma lengthening as expected as air is ionized and incorporated into the plasma. Note that this growth would not occur in a railgun experiment where the plasma armature is pushing a solid object.

The precursor length is also increasing due to plasma air mixing. However, the precursor does not include all the swept-up gas, as evidenced by the last column of Table B-1. This final column, labeled *shock front*, is the calculated distance of the shock front from the plasma armature. It is calculated by dividing the distance traveled by the plasma armature from its starting point times the compression ratio $(\gamma + 1)/(\gamma - 1) = 6$. Initially, this length and the precursor length are comparable. However, as motion proceeds, the nonconducting, shocked gas accumulates—eventually extending ~200 mm in front of the precursor.

From this analysis, we conclude the following:

1. The constant length of the plasma tail shows that the alumina bore insulators are not ablating and adding material to the plasma.
2. The observed growth of the plasma length is consistent with the expected interaction of the plasma with the shocked air being swept up.

* In reality, ablation is never entirely absent because there is a small amount of copper vaporized from the rails as an intrinsic part of the current emission process. This small mass is ionized and merged with the armature.

Appendix C: Summary of Pre-Injector Subsystem Development

Pre-acceleration is necessary in plasma-armature launchers because the effects of slow-moving arcs are quite damaging to bore components. In 2006, we designed, built, and tested a plasma-driven pre-injector to accelerate 7 g polycarbonate projectiles to 800–1000 m/s.

Our pre-injector, shown in Figures C1 and C2, is similar to plasma-source capillary generators used in electrothermal chemical (ETC) launchers. The pre-injector consists of a 30 cm long, 20 mm inner diameter polyethylene liner contained within a steel pressure vessel. The chamber is evacuated to < 10 Torr. An arc discharge is initiated by discharging a > 100 kA current into a 0.001 inch diameter aluminum wire that connects the cathode and the anode. This causes the wire to explode within the first few microseconds of the pulse. For the remainder of the current pulse (~100 μs), a plasma arc is sustained between the cathode and the anode. The arc vaporizes a controlled amount of polyethylene from the liner and rapidly heats it to high temperature. The resulting gas, at a pressure of 1–2 × 10^8 Pa, accelerates the projectile, which is initially at rest at the entrance to the barrel.

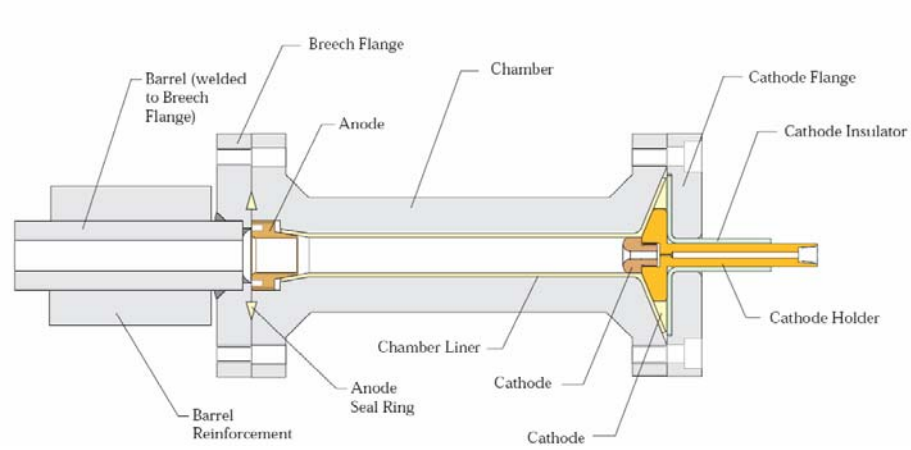

Figure C1. Schematic of the pre-injector chamber and barrel.

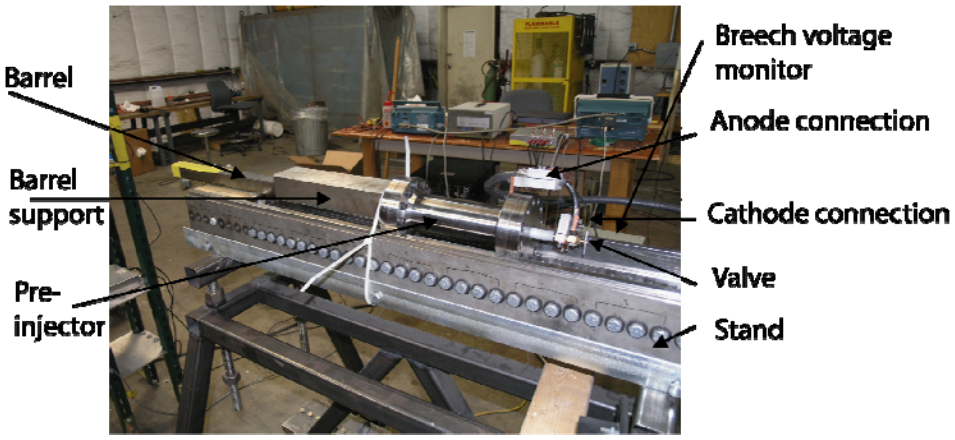

Figure C2. Pre-injector system overview.

To drive the pre-injector, we designed and built a power supply capable of providing 200 kA pulses with a 50 μs rise time and a *FWHM* of roughly 100 μs. Photos and a schematic of the power supply are shown in Figures C3 through C5. To achieve a high level of energy conversion, a design objective was a critically damped system that makes the pulse waveform as square as possible while minimizing the current decay time once the projectile has been accelerated through the barrel. To this end, the power supply uses six 206 μF capacitors with a rated charge voltage of 21 kV. Each capacitor has a 300 mΩ high-energy-density resistor connected at its positive terminal, which acts to critically damp the system as well as fuse the system in the event of a capacitor failure. An additional feature of this system resistance is that it reduces the inductance needed to achieve critical damping to only 1.5 μH. This inductance was easily provided by the stray inductance of the system cabling and bus work, thus eliminating the need to construct an additional inductor.

Figure C3. Overall view of the pre-injector power supply.

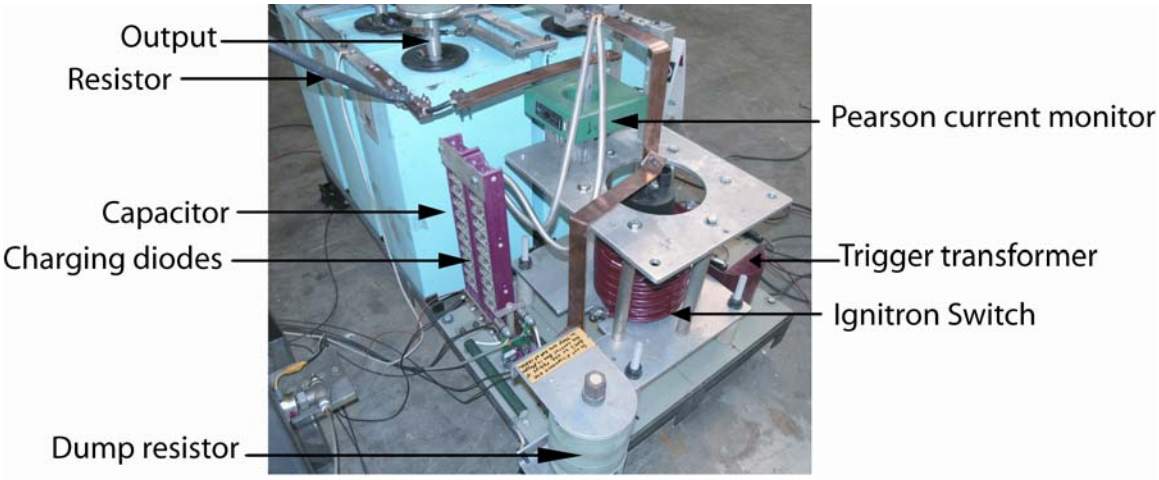

Figure C4. Close-up view of the pre-injector power supply.

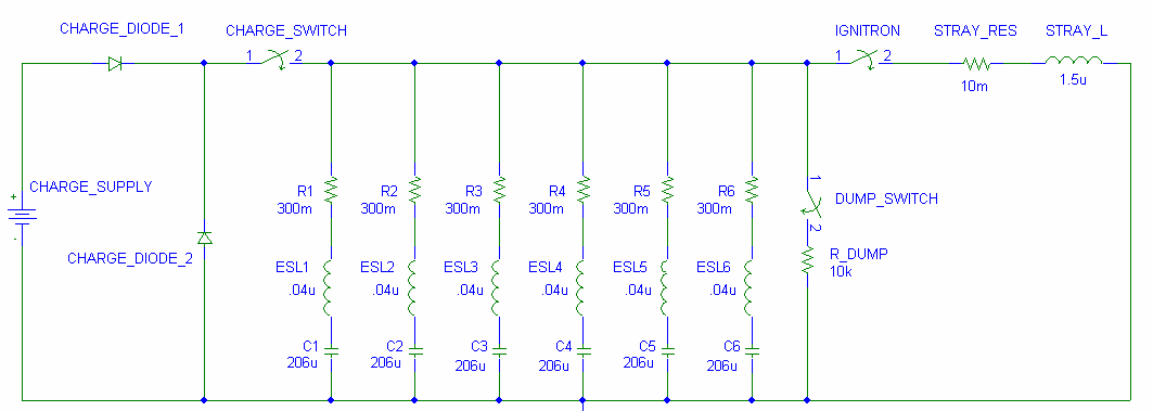

Figure C5. Schematic of the pre-injector power supply.

Testing

We performed several tests of the entire pre-injection system with good results. We summarize here the results from two of the tests to provide a sense for how the system performs. The first test to be discussed was performed with the capacitors charged to 10 kV. Figure C6 displays the current and breech voltage waveforms. As shown in the figure, the peak current and breech voltage are roughly 90 kA and 6 kV respectively. The initial voltage spike represents the exploding of the wire and formation of a plasma arc in the chamber. Integrating the product of *I* times *V* gives the total energy input to the capillary of 39 kJ, with 90 percent of this energy deposited in 150 μs. The plasma arc extinguishes after about 400 μs, leaving about 800 V residual charge on the capacitors.

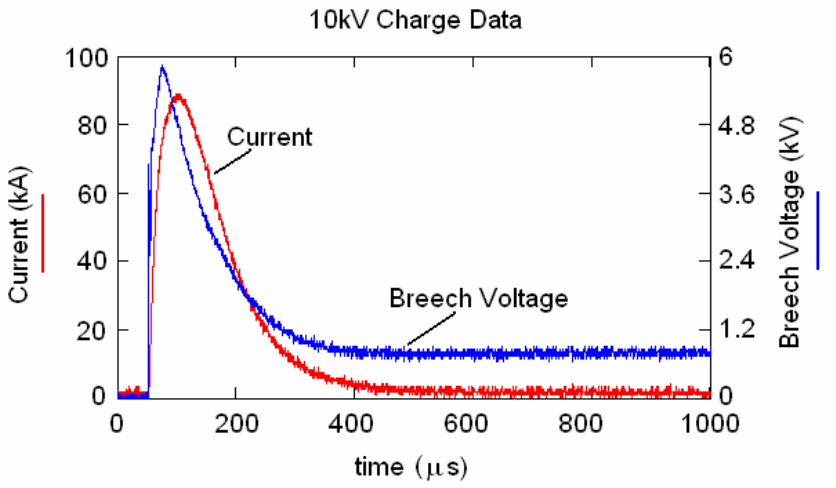

Figure C6. Diagnostic waveforms.

By dividing the breech voltage waveform by the current waveform, the plasma impedance can be calculated as shown in Figure C7. The plasma impedance is shown to be roughly 50 mΩ during steady plasma generation. In order to verify this measurement, the schematic shown above was simulated with an additional 50 mΩ added into the circuit and compared with the measured data. A good agreement between simulated and measured data was observed, as shown in Figure C8.

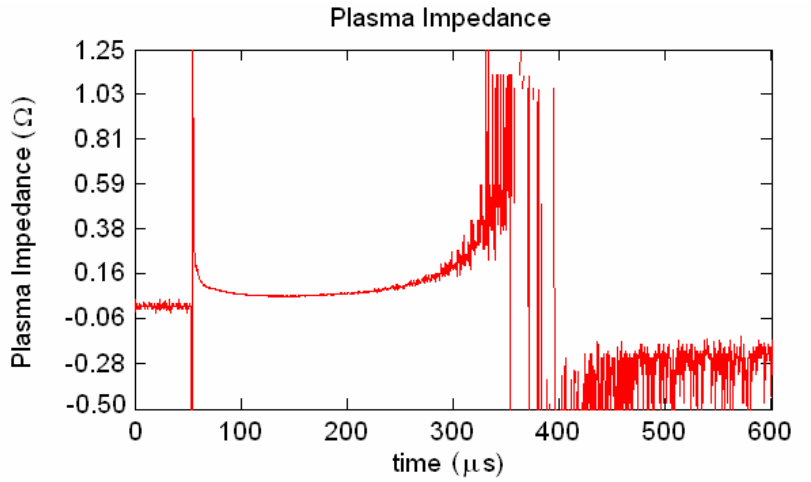

Figure C7. Plasma impedance found from dividing the current trace into the voltage trace.

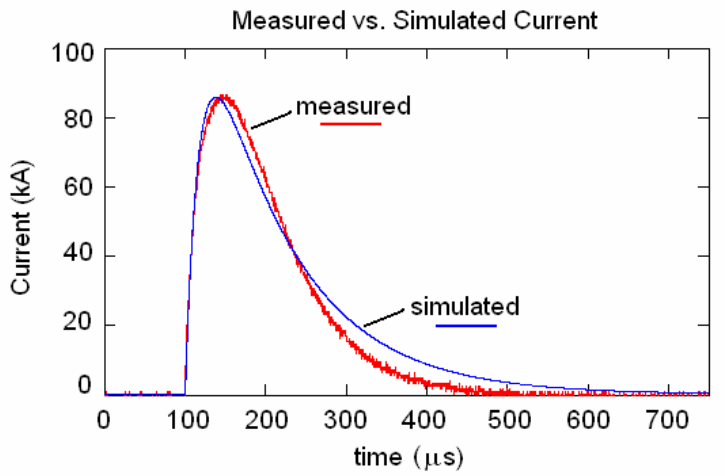

Figure C8. Comparison of the simulated and measured current waveforms.

The velocity of the projectile in these tests was measured using two break screens located about a meter away from the muzzle. The break screens and their mounting fixture are shown in Figure C9. The velocity is calculated by dividing the screen separation of 28.9 cm by time difference between break-screen signals, as shown in Figure C10. This test, conducted at 10 kV charge voltage, produced a projectile velocity of 688 m/s. Our fastest tests, conducted at 14 kV, resulted in a velocity of 812 m/s. The peak current applied was 128 kA, and the plasma impedance was 38 mΩ during steady plasma generation.

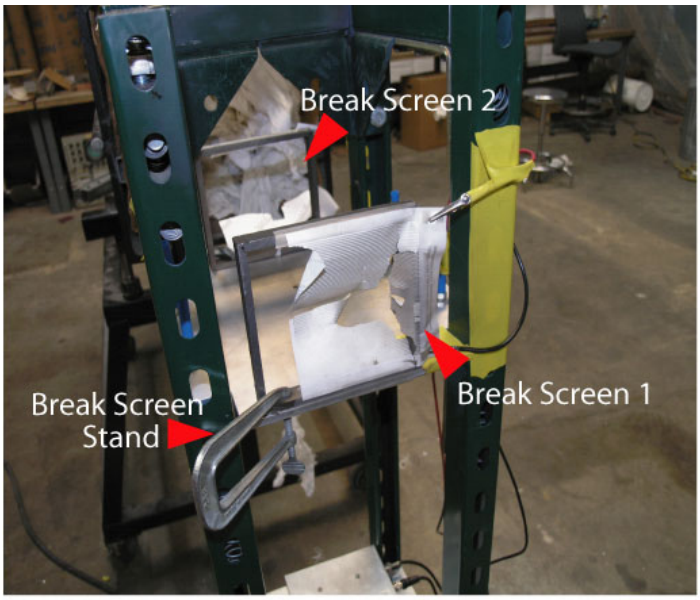

Figure C9. Break Screen Setup.

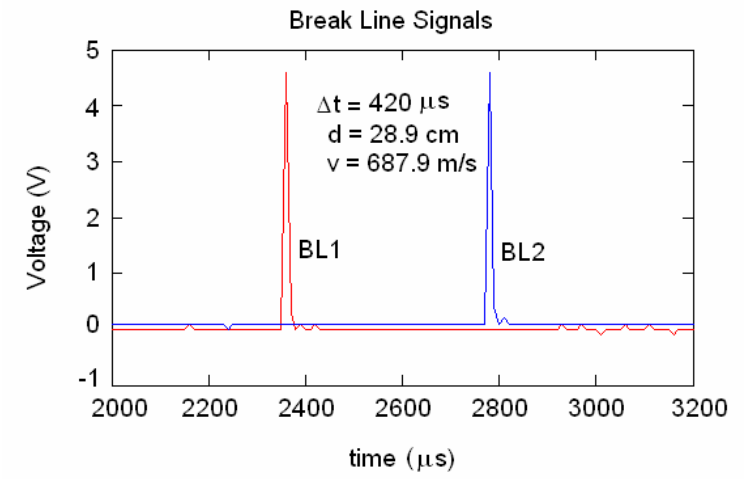

Figure C10. Break Line Signals.

Although the plasma injector operates well, the peak injection speed of 800 m/s is at the low end of the desirable range. To achieving the goal of 1,000 m/s we intend to lengthen the pre-injector plasma chamber and barrel. A new pre-injector is currently in fabrication that has a chamber length of 38.1 cm and barrel length of 91.4 cm as opposed to the current design which has a chamber length of 22.8 cm and barrel length of 76.2 cm. These modifications should result in higher plasma impedance, which will improve coupling of energy from the power supply to the projectile.